

# A model of hardness and fracture toughness of solids

Cite as: J. Appl. Phys. **126**, 125109 (2019); <https://doi.org/10.1063/1.5113622>

Submitted: 05 June 2019 . Accepted: 30 August 2019 . Published Online: 25 September 2019

Efim Mazhnik , and Artem R. Oganov 



View Online



Export Citation



CrossMark

## Lock-in Amplifiers up to 600 MHz

starting at

\$6,210



 Zurich  
Instruments

Watch the Video



AIP  
Publishing

# A model of hardness and fracture toughness of solids

Cite as: J. Appl. Phys. **126**, 125109 (2019); doi: [10.1063/1.5113622](https://doi.org/10.1063/1.5113622)

Submitted: 5 June 2019 · Accepted: 30 August 2019 ·

Published Online: 25 September 2019



View Online



Export Citation



CrossMark

Efim Mazhnik<sup>1,a)</sup>  and Artem R. Oganov<sup>1,2,3,b)</sup> 

## AFFILIATIONS

<sup>1</sup>Skolkovo Institute of Science and Technology, Skolkovo Innovation Center, 3 Nobel Street, Moscow 121205, Russia

<sup>2</sup>Moscow Institute of Physics and Technology, 9 Institutsky Lane, Dolgoprudny 141700, Russia

<sup>3</sup>International Center for Materials Discovery, Northwestern Polytechnical University, Xi'an 710072, China

**Note:** This paper is part of the Special Topic on Ultra-Hard Materials.

<sup>a)</sup>Electronic mail: [efim.mazhnik@skoltech.ru](mailto:efim.mazhnik@skoltech.ru)

<sup>b)</sup>Electronic mail: [a.oganov@skoltech.ru](mailto:a.oganov@skoltech.ru)

## ABSTRACT

Hardness and fracture toughness are some of the most important mechanical properties. Here, we propose a simple model that uses only the elastic properties to calculate the hardness and fracture toughness. Its accuracy is checked by comparison with other available models and experimental data for metals, covalent and ionic crystals, and bulk metallic glasses. We found the model to perform well on all datasets for both hardness and fracture toughness, while for auxetic materials (i.e., those having a negative Poisson's ratio), it turned out to be the only model that gives reasonable hardness. Predictions are made for several materials for which no experimental data exist.

Published under license by AIP Publishing. <https://doi.org/10.1063/1.5113622>

## I. INTRODUCTION

Hardness is the material's resistance to local deformation induced by pressing a harder solid (indenter). It can be characterized by various scales depending on the method of measurement. The most common scales are Brinell hardness (HB), Rockwell hardness (HRC), Knoop hardness (HK), and Vickers hardness (HV). These hardness scales are widely used in standardized tests in engineering and metallurgy.

Fracture toughness  $K_{IC}$  characterizes the ability of a material to resist propagation of a fracture. Quantitatively, it can be determined from the stress intensity factor  $K$  at which a thin crack in the material begins to grow.

Both of these characteristics are very important in materials science. For example, materials used in drilling and cutting technologies require both high hardness and fracture toughness. However, the values are often quite difficult to measure accurately because the applied stress can depend on a variety of factors including the orientation of the material, the loading forces, and the geometry of an indenter. Hardness and fracture toughness depend on grain size,<sup>1</sup> presence of defects, conditions of loading, etc. As a result, the experimental values of hardness can vary by much more than 10%<sup>2</sup> for the same material.

Accurate models of hardness and fracture toughness would be useful for designing experiments and for the computational design of new materials.<sup>3</sup> Since these areas are usually demanding for computational resources, models, which could allow fast and simple estimation of the properties, are of particular interest.

Therefore, there had been many attempts to establish correspondence between hardness and fracture toughness with the elastic properties of materials, because they are easier to measure and many experimental data are already available. Although hardness and fracture toughness are not purely elastic phenomena, there are two big reasons why a good correlation can be established. The first one is that many materials are brittle and fail in or near the elastic regime. The second one is that all of these parameters are functions of material structure and if some parameter or their combinations give sufficiently different values for several classes of materials, it can be a strong predictor of the other properties including those connected with plastic behavior.

The first successful model of such a type was proposed by Teter,<sup>4</sup> who found that the relationship between the hardness and shear modulus is approximately linear (Fig. 1).

Although this correlation works quite well for particular classes of materials, using the shear modulus alone to predicting

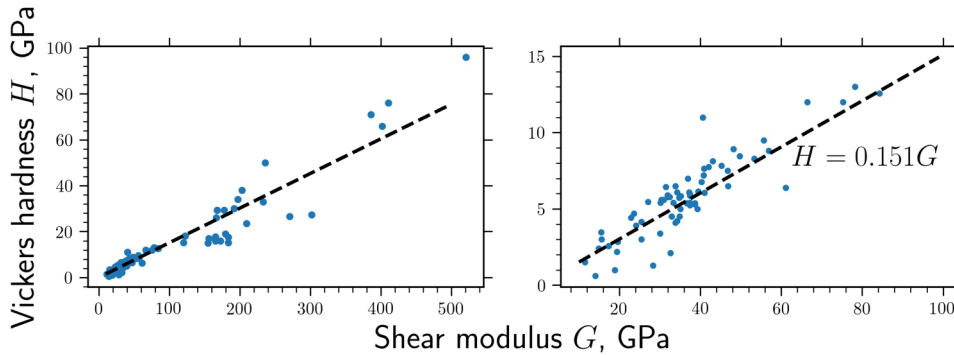


FIG. 1. Correlation between experimental Vickers hardness  $H$  and shear modulus  $G$  on different scales. The dashed line denotes the theoretical coefficient obtained in Ref. 5.

the hardness has its limitations. For example, the shear modulus of  $B_6O$  is about the same as that of TiN, while its hardness is about 1.5 times higher.

Chen *et al.*<sup>5</sup> proposed to use the bulk modulus  $B$  together with the shear modulus  $G$  to predict hardness. They obtained the following formula by fitting the experimental data on crystalline materials:

$$H = 2 \left( \frac{G^3}{B^2} \right)^{0.585} - 3. \quad (1)$$

For this expression to work correctly,  $G$ ,  $B$ , and  $H$  must be expressed in gigapascals. This model, while working quite well for a wide class of materials, also has certain limitations. For instance, it overestimates the hardness of materials that have low or negative Poisson's ratio. Besides, it incorrectly predicts the hardness for unusually hard materials like  $OsB_2$  and can give unphysical negative hardness values for soft compounds.

There are also models that attempt to calculate the hardness from the chemical bond properties. For example, in Gao's<sup>6</sup> model, the hardness depends mainly on the bond length, average electron density, and ionicity. Šimůnek and Vackář's<sup>7</sup> model uses the chemical bond strength. Li *et al.*<sup>8</sup> use the electronegativities, covalent radii, and the bond length, and Lyahov-Oganov model<sup>9</sup> augments it with the bond-valence model and graph theory.

A reliable model of fracture toughness was proposed by Niu *et al.*<sup>10</sup> who used the following empirical formula to calculate the fracture toughness of insulators and semiconductors:

$$K_{IC} = V_0^{1/6} G(B/G)^{1/2}, \quad (2)$$

where  $V_0$  is the volume per atom.

For pure metals and intermetallic compounds, they introduced an enhancement factor  $\alpha$ :

$$\alpha = 43g(E_F)_R^{1/4} f_{EN}, \quad (3)$$

where  $g(E_F)_R$  is the density of states at the Fermi level relative to the free electron gas, and the electronegativity factor  $f_{EN}$  equals 1 for pure metals, while for binary compounds  $A_mB_n$ , it is determined as

$$f_{EN} = \beta \left/ \left[ 1 + \frac{C_m^1 C_n^1}{C_{m+n}^2} \sqrt{\frac{(\chi_A - \chi_B)^2}{\chi_A \chi_B}} \right]^\gamma \right., \quad (4)$$

where  $C_m^1$ ,  $C_n^1$ , and  $C_{m+n}^2$  are binomial coefficients, and  $\chi_A$  and  $\chi_B$  are the Allen electronegativities<sup>11</sup> of the elements. The parameters  $\beta$  and  $\gamma$  are obtained by fitting the experimental data.

The resulting fracture toughness is then determined as

$$K_{IC} = (1 + \alpha) V_0^{1/6} G(B/G)^{1/2}. \quad (5)$$

## II. MODEL AND RESULTS

### A. Hardness

Among the different scales of hardness, we chose the Vickers hardness because it is one of the most convenient, is widely used in tests, and many experimental data are available. It can be used for most solid materials, has a well defined numerical scale, and the variance of the values in different experimental settings is often small compared to other methods.

Experimentally, the procedure consists of applying a diamond load in the form of a square-based pyramid into the sample and

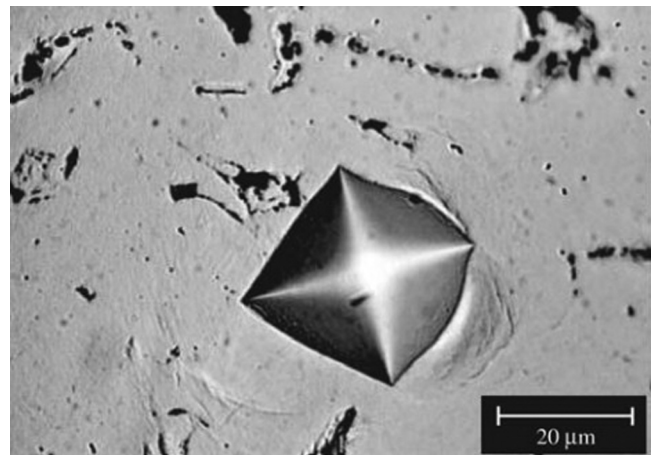
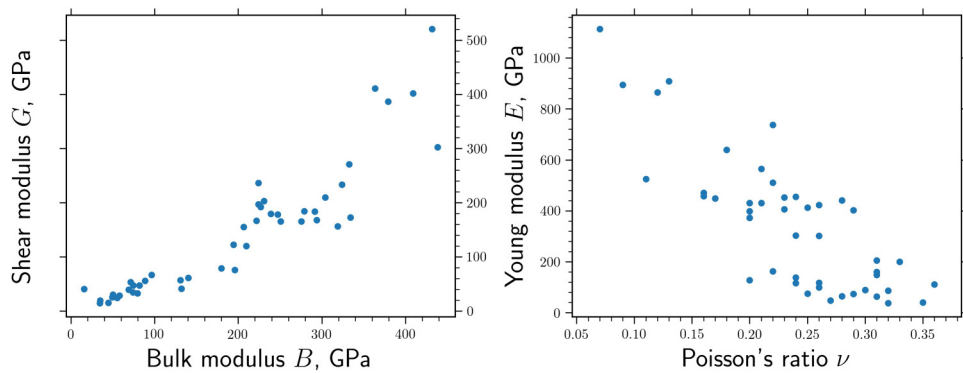
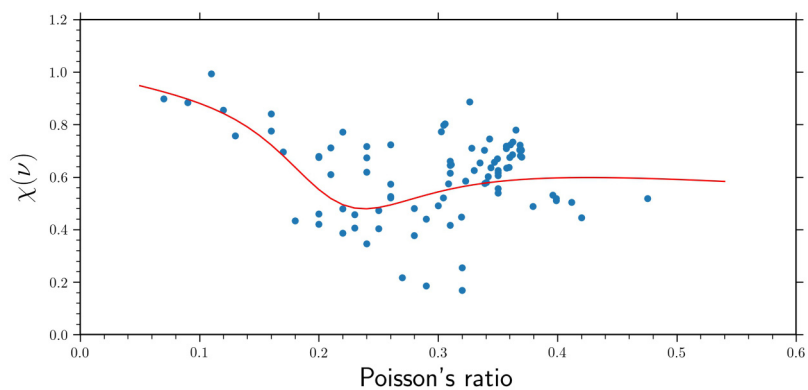


FIG. 2. A microscopic image of indentation on a metallic surface from a Vickers hardness test obtained from Franco *et al.*, Mater. Res. 7(3), 483491 (2004).<sup>12</sup> Copyright 2004 Author(s), licensed under a Creative Commons Attribution (CC BY) license.



**FIG. 3.** Experimental data for the shear modulus  $G$  vs bulk modulus  $B$  and Young's modulus  $E$  vs Poisson's ratio  $\nu$  for covalent and ionic crystals (Table I).



**FIG. 4.** Plot and fitting of  $\chi(\nu)$  for experimental data for covalent and ionic crystals and bulk metallic glasses (Tables I and II).

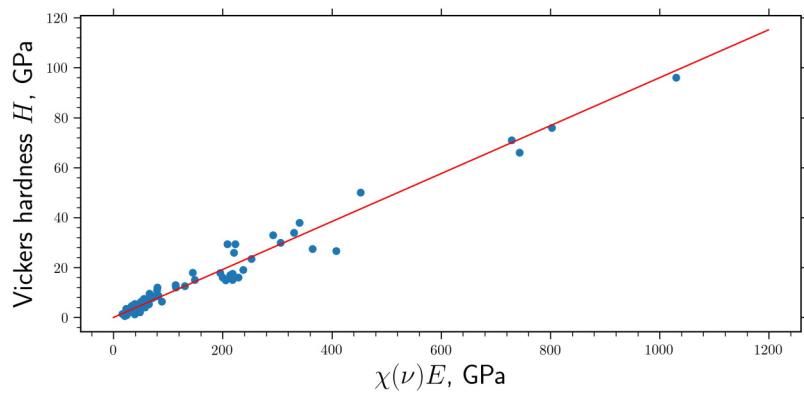


**FIG. 5.** Plot of Vickers hardness  $H$  vs  $\chi(\nu)E$  for experimental data for covalent and ionic crystals and bulk metallic glasses (Tables I and II).

**TABLE I.** Comparison between experimental hardness and hardness predicted by the current model and models of Chen,<sup>5</sup> Gao,<sup>6</sup> and Simunek<sup>7</sup> for covalent and ionic crystals. The elastic properties are calculated within the framework of density functional theory using the Perdew, Burke, and Ernzerhof (PBE) exchange-correlation functional<sup>13</sup> within the generalized gradient approximation and the projector-augmented wave method<sup>14</sup> as implemented in the Vienna *Ab Initio* Simulation Package (VASP).<sup>15,16</sup> The calculated Young's modulus  $E$  and Poisson's ratio  $\nu$  are determined within the Voigt-Reuss-Hill approximation.<sup>17</sup> Root Mean Square Error (RMSE) and Mean Absolute Error (MAE) are provided for the comparison.

Material	Young's modulus $E$ (GPa)	Poisson's ratio $\nu$	$H_V^{\text{exp}}$ (GPa)	$H_V^{\text{calc}}$ (GPa)	$H_V^{\text{Chen}}$ (GPa)	$H_V^{\text{Gao}}$ (GPa)	$H_V^{\text{Simunek}}$ (GPa)
Diamond	1114	0.07	96.0 <sup>18</sup>	98.9	93.6	93.6	95.4
BC <sub>2</sub> N	895	0.09	76.0 <sup>4</sup>	77.1	76.5	78.0	71.9
BC <sub>5</sub>	865	0.12	71.0 <sup>19</sup>	70.0	63.6	...	...
c-BN	908	0.13	66.0 <sup>20</sup>	71.4	62.4	64.5	63.2
$\gamma$ -B <sub>28</sub>	524	0.11	50.0 <sup>21</sup>	43.4	49.0	...	...
B <sub>4</sub> C	449	0.17	30.0 <sup>22,a</sup>	29.4	32.6	...	...
B <sub>6</sub> O	471	0.16	38.0 <sup>23</sup>	32.7	35.5	...	...
$\beta$ -SiC	457	0.16	34.0 <sup>24</sup>	31.7	34.8	30.3	31.1
SiO <sub>2</sub> (stishovite)	564	0.21	33.0 <sup>4</sup>	28.1	30.0	30.4	...
WC	737	0.22	27.4 <sup>25</sup>	35.0	33.5	26.4	21.5
OsB <sub>2</sub>	423	0.26	29.4 <sup>26</sup>	20.0	17.8	22.8	26.7
VC	511	0.22	23.5 <sup>27</sup>	24.3	26.5	...	27.2
ReB <sub>2</sub>	639	0.18	26.6 <sup>28</sup>	39.1	38.6	23.7	28.2
ZrC	399	0.20	26.0 <sup>29</sup>	21.2	25.5	...	...
TiC	430	0.21	29.4 <sup>30,b</sup>	21.4	25.1	...	18.8
HfC	430	0.20	19.0 <sup>29</sup>	22.8	26.7	...	...
AlN	303	0.24	18.0 <sup>24</sup>	13.9	16.3	21.7	17.7
Al <sub>2</sub> O <sub>3</sub>	406	0.23	17.8 <sup>31</sup>	18.8	21.3	20.6	...
TiN	452	0.23	17.6 <sup>30,b</sup>	20.9	22.9	...	18.7
NbN	402	0.29	17.0 <sup>32</sup>	20.5	13.6	...	19.5
NbC	441	0.28	16.0 <sup>33</sup>	22.0	15.7	...	18.3
HfN	413	0.25	16.0 <sup>32</sup>	19.2	18.8	...	...
GaN	302	0.26	15.1 <sup>34</sup>	14.3	14.1	18.1	18.5
RuB <sub>2</sub>	455	0.24	15.1 <sup>28</sup>	20.9	21.5	15.1	...
BeO	372	0.20	15.0 <sup>35</sup>	19.7	24.3	12.7	...
ZrO <sub>2</sub>	205	0.31	13.0 <sup>20</sup>	10.9	6.7	10.8	...
ZrN	200	0.33	12.0 <sup>32</sup>	11.0	5.2	...	...
Si	162	0.22	12.0 <sup>36</sup>	7.7	12.0	13.6	11.3
GaP	138	0.24	9.5 <sup>24,b</sup>	6.3	9.2	8.9	8.7
InN	149	0.31	8.8 <sup>37</sup>	7.9	5.0	10.4	8.2
Ge	128	0.20	8.3 <sup>38</sup>	6.8	11.6	11.7	9.7
GaAs	116	0.24	7.5 <sup>24,b</sup>	5.3	8.0	8.0	7.4
ZnO	111	0.36	7.2 <sup>39</sup>	6.3	1.4	...	...
Y <sub>2</sub> O <sub>3</sub>	160	0.31	6.4 <sup>40</sup>	8.5	5.4	7.7	...
AlP	118	0.26	6.5 <sup>24,c</sup>	5.6	6.9	9.6	7.9
InP	89	0.30	4.2 <sup>24,b</sup>	4.6	3.4	6.0	5.1
AlAs	99	0.26	5.0 <sup>2</sup>	4.7	5.9	8.5	6.8
GaSb	63	0.31	3.9 <sup>24,b</sup>	3.4	1.9	6.0	5.6
AlSb	75	0.25	3.4 <sup>41</sup>	3.5	5.0	4.9	4.9
InAs	65	0.28	3.0 <sup>24,b</sup>	3.2	3.1	5.7	4.5
InSb	40	0.35	2.4 <sup>42,b</sup>	2.2	0.0 <sup>c</sup>	4.3	3.6
ZnS	86	0.32	2.1 <sup>43,d</sup>	4.6	2.4	6.8	2.7
ZnSe	73	0.29	1.3 <sup>44,d</sup>	3.7	3.1	5.5	2.6
ZnTe	48	0.27	1.0 <sup>44,d</sup>	2.3	2.5	4.1	2.3
CdTe	37	0.32	0.6 <sup>44,d</sup>	2.0	0.3	...	...
RMSE				4.1	4.4	2.8	2.9
MAE				3.1	3.2	2.5	2.1

<sup>a</sup>There are reports that this value can reach 41 (summarized in Ref. 22). However, we use the average value as stated in Ref. 4.

<sup>b</sup>Some authors incorrectly use the Knoop hardness values for these materials which are provided in Refs. 6 and 7 from Refs. 2 and 45 instead of the Vickers hardness.

<sup>c</sup>Estimated from the known values of Knoop hardness (9.5 GPa in Ref. 2) and Mohs hardness (5.5 in Ref. 46).

<sup>d</sup>There is a very apparent anisotropy for the microhardness for these cubic compounds.<sup>47</sup> The values are provided for the polycrystalline form  $H$  (polycrystalline)  $\approx H(111) > H(110)$ .

<sup>e</sup>Here, Chen's model gives a negative value. Zero value was assigned to maintain physical meaning.

**TABLE II.** Comparison between experimental hardness and hardness predicted by the current model and model of Chen<sup>5</sup> for bulk metallic glasses. Note that Chen *et al.* used another formula to calculate the hardness, whereas our formula is the same for crystals and glasses. The elastic properties are calculated using the experimental shear modulus  $G$  and bulk modulus  $B$  (Ref. 5) using the homogeneous approximation.

Material	Young's modulus $E$ (GPa)	Shear modulus $G$ (GPa)	Poisson's ratio $\nu$	$H_v^{\text{exp}}$ (GPa)	$H_v^{\text{calc}}$ (GPa)	$H_v^{\text{Chen}}$ (GPa)
Fe <sub>41</sub> Co <sub>7</sub> Cr <sub>15</sub> Mo <sub>14</sub> C <sub>15</sub> B <sub>6</sub> Y <sub>2</sub> <sup>48</sup>	226	84	0.34	12.6	12.5	12.7
Ni <sub>50</sub> Nb <sub>50</sub> <sup>49</sup>	132	48	0.37	8.9	7.5	7.3
Ni <sub>40</sub> Cu <sub>5</sub> Ti <sub>17</sub> Zr <sub>28</sub> Al <sub>10</sub> <sup>50</sup>	134	50	0.35	8.5	7.5	7.5
Ni <sub>39.8</sub> Cu <sub>5.97</sub> Ti <sub>15.92</sub> Zr <sub>27.86</sub> Al <sub>9.95</sub> Si <sub>0.5</sub> <sup>50</sup>	117	43	0.36	8.1	6.6	6.5
Ni <sub>40</sub> Cu <sub>5</sub> Ti <sub>16.5</sub> Zr <sub>28.5</sub> Al <sub>10</sub> <sup>50</sup>	122	45	0.35	7.8	6.8	6.8
Ni <sub>45</sub> Ti <sub>20</sub> Zr <sub>25</sub> Al <sub>10</sub> <sup>50</sup>	114	42	0.36	7.8	6.4	6.3
Ni <sub>40</sub> Cu <sub>6</sub> Ti <sub>16</sub> Zr <sub>28</sub> Al <sub>10</sub> <sup>50</sup>	111	41	0.36	7.7	6.2	6.2
{Zr <sub>41</sub> Ti <sub>14</sub> Cu <sub>12.5</sub> Ni <sub>10</sub> Be <sub>22.5</sub> } <sub>98</sub> Y <sub>2</sub> <sup>51</sup>	108	40	0.33	6.8	5.9	6.1
Zr <sub>54</sub> Al <sub>15</sub> Ni <sub>10</sub> Cu <sub>19</sub> Y <sub>2</sub> <sup>51</sup>	92	34	0.36	6.5	5.2	5.1
Zr <sub>53</sub> Al <sub>14</sub> Ni <sub>10</sub> Cu <sub>19</sub> Y <sub>4</sub> <sup>51</sup>	86	32	0.46	6.4	4.9	4.8
Zr <sub>41</sub> Ti <sub>14</sub> Cu <sub>12.5</sub> Ni <sub>8</sub> Be <sub>22.5</sub> C <sub>1</sub> <sup>51</sup>	106	40	0.34	6.1	5.9	6.0
Zr <sub>46.75</sub> Ti <sub>8.25</sub> Cu <sub>7.5</sub> Ni <sub>10</sub> Be <sub>27.5</sub> <sup>49</sup>	100	37	0.34	6.1	5.6	5.6
Zr <sub>48</sub> Nb <sub>8</sub> Cu <sub>14</sub> Ni <sub>12</sub> Be <sub>18</sub> <sup>51</sup>	94	34	0.37	6.1	5.3	5.2
Zr <sub>34</sub> Ti <sub>15</sub> Cu <sub>10</sub> Ni <sub>11</sub> Be <sub>28</sub> Y <sub>2</sub> <sup>51</sup>	110	41	0.34	6.1	6.1	6.2
Zr <sub>57</sub> Nb <sub>5</sub> Cu <sub>15.4</sub> Ni <sub>12.6</sub> Al <sub>10</sub> <sup>49</sup>	87	32	0.37	5.9	4.9	4.8
Zr <sub>48</sub> Nb <sub>8</sub> Cu <sub>12</sub> Fe <sub>8</sub> Be <sub>24</sub> <sup>51</sup>	96	35	0.36	5.9	5.5	5.3
Zr <sub>40</sub> Ti <sub>15</sub> Cu <sub>11</sub> Ni <sub>11</sub> Be <sub>21.5</sub> Y <sub>1</sub> Mg <sub>0.5</sub> <sup>51</sup>	94	35	0.36	5.7	5.3	5.2
Zr <sub>41</sub> Ti <sub>14</sub> Cu <sub>12.5</sub> Ni <sub>10</sub> Be <sub>22.5</sub> <sup>49</sup>	101	37	0.35	6.0	5.7	5.6
Zr <sub>65</sub> Al <sub>10</sub> Ni <sub>10</sub> Cu <sub>15</sub> <sup>49</sup>	83	31	0.35	5.6	4.7	4.6
Zr <sub>57</sub> Ti <sub>5</sub> Cu <sub>20</sub> Ni <sub>8</sub> Al <sub>10</sub> <sup>49</sup>	82	30	0.36	5.4	4.6	4.6
Cu <sub>60</sub> Hf <sub>10</sub> Zr <sub>20</sub> Ti <sub>10</sub> <sup>49</sup>	101	37	0.35	7.0	5.7	5.6
Cu <sub>50</sub> Zr <sub>50</sub> <sup>49</sup>	85	32	0.33	5.8	4.8	4.8
Pd <sub>40</sub> Ni <sub>40</sub> P <sub>20</sub> <sup>49</sup>	108	39	0.42	5.4	6.2	5.7
Pd <sub>40</sub> Ni <sub>10</sub> Cu <sub>30</sub> P <sub>20</sub> <sup>49</sup>	98	35	0.40	5.0	5.6	5.3
Pd <sub>77.5</sub> Si <sub>16.5</sub> Cu <sub>6</sub> <sup>49</sup>	95	34	0.38	4.5	5.4	5.3
Pt <sub>60</sub> Ni <sub>15</sub> P <sub>25</sub> <sup>49</sup>	96	34	0.40	4.1	5.5	5.1
Mg <sub>65</sub> Cu <sub>25</sub> Tb <sub>10</sub> <sup>49</sup>	51	20	0.31	2.8	2.7	3.0
Nb <sub>60</sub> Al <sub>10</sub> Fe <sub>20</sub> Co <sub>10</sub> <sup>49</sup>	51	19	0.32	2.2	2.8	2.9
Ce <sub>70</sub> Al <sub>10</sub> Ni <sub>10</sub> Cu <sub>10</sub> <sup>49</sup>	30	12	0.30	1.5	1.6	1.7
Er <sub>55</sub> Al <sub>25</sub> Co <sub>20</sub> <sup>52</sup>	71	27	0.31	5.5	3.7	4.1
Dy <sub>55</sub> Al <sub>25</sub> Co <sub>20</sub> <sup>52</sup>	61	24	0.30	4.7	3.2	3.6
Tb <sub>55</sub> Al <sub>25</sub> Co <sub>20</sub> <sup>52</sup>	60	23	0.30	4.4	3.1	3.5
Ho <sub>55</sub> Al <sub>25</sub> Co <sub>20</sub> <sup>52</sup>	67	25	0.31	4.1	3.5	3.8
La <sub>55</sub> Al <sub>25</sub> Co <sub>20</sub> <sup>52</sup>	41	15	0.34	3.5	2.2	2.3
La <sub>55</sub> Al <sub>25</sub> Cu <sub>10</sub> Ni <sub>5</sub> Co <sub>5</sub> <sup>52</sup>	42	16	0.34	3.0	2.3	2.4
Pr <sub>55</sub> Al <sub>25</sub> Co <sub>20</sub> <sup>52</sup>	46	17	0.32	2.6	2.5	2.6
RMSE					0.9	0.9
MAE					0.8	0.8

**TABLE III.** Comparison between hardness predicted by the current model and models of Chen<sup>5</sup> and Gao<sup>6</sup> for auxetic materials found in Ref. 53 by computational search. Experimental data are available only for  $\alpha$ -SiO<sub>2</sub>. Apparently, all other models significantly overestimate hardness of these materials. Elastic properties are calculated within the framework of density functional theory using the Perdew, Burke, and Ernzerhof (PBE) exchange-correlation functional<sup>13</sup> within the generalized gradient approximation and the projector-augmented wave method<sup>14</sup> as implemented in the Vienna *Ab Initio* Simulation Package (VASP).<sup>15,16</sup> The calculated Young's modulus  $E$  and Poisson's ratio  $\nu$  are determined within the Voigt-Reuss-Hill approximation.<sup>17</sup>

Material	Young's modulus $E$ (GPa)	Poisson's ratio $\nu$	$H_v^{\text{exp}}$ (GPa)	$H_v^{\text{calc}}$ (GPa)	$H_v^{\text{Chen}}$ (GPa)	$H_v^{\text{Gao}}$ (GPa)
$\alpha$ -SiO <sub>2</sub>	65	-0.20	11.0 <sup>2</sup>	7.7	51.0	30.6 <sup>a</sup>
o-AlPO <sub>4</sub> <sup>b</sup>	44	-0.28	...	5.7	55.7	...
FeV <sub>3</sub> O <sub>8</sub>	23	-0.07	...	2.4	14.8	...
CoV <sub>3</sub> O <sub>8</sub>	21	-0.04	...	2.1	12.0	...

<sup>a</sup>Value is obtained from Ref. 6 and it is mentioned that not all factors are considered in the model due to the open crystal structure of this compound.

<sup>b</sup>For high-temperature orthorhombic phase, see Ref. 54.

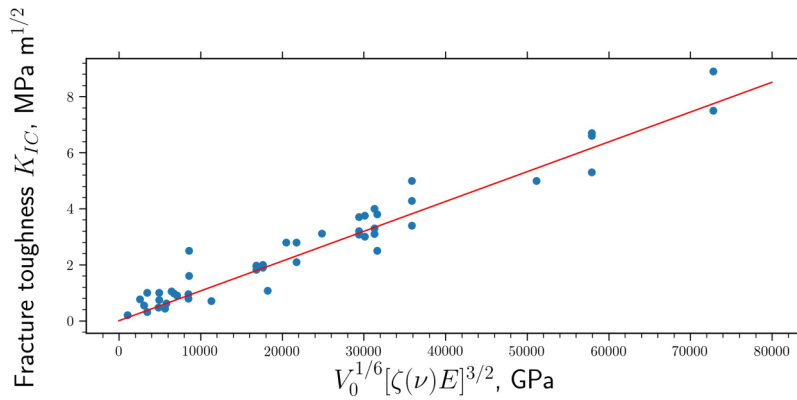


**FIG. 6.** Plot of fracture toughness  $K_{IC}$  vs  $V_0^{1/6} [\zeta(\nu)E]^{3/2}$  for experimental data for covalent and ionic crystals (Table IV).

**TABLE IV.** Comparison between experimental fracture toughness  $K_{IC}$  and fracture toughness predicted by the current model and other models for covalent and ionic crystals. The elastic properties and volume per atom  $V_0$  are calculated within the framework of density functional theory using the Perdew, Burke, and Ernzerhof (PBE) exchange-correlation functional<sup>13</sup> within the generalized gradient approximation and the projector-augmented wave method<sup>14</sup> as implemented in the Vienna *Ab Initio* Simulation Package (VASP).<sup>15,16</sup> The calculated Young's modulus  $E$  and Poisson's ratio  $\nu$  are determined within the Voigt-Reuss-Hill approximation.<sup>17</sup>

Material	Young's modulus $E$ (GPa)	Poisson's ratio $\nu$	$V_0$ ( $\text{\AA}^3/\text{atom}$ )	$K_{IC}^{\text{exp}}$ ( $\text{MPa m}^{1/2}$ )	$K_{IC}^{\text{calc}}$ ( $\text{MPa m}^{1/2}$ )	$K_{IC}^{\text{Niu}}$ ( $\text{MPa m}^{1/2}$ )
Diamond	1114	0.07	5.70	5.3–6.7 <sup>55</sup>	6.2	6.3
WC	737	0.22	10.61	7.5 <sup>55</sup>	7.7	5.4
c-BN	908	0.13	5.95	5.0 <sup>55</sup>	5.4	5.4
TiN	452	0.23	9.66	3.4–5.0 <sup>55</sup>	3.8	3.3
TiC	430	0.21	10.19	2.0–3.8 <sup>55</sup>	3.4	3.1
$\beta$ -SiC	457	0.16	10.49	3.1–4.0 <sup>55</sup>	3.3	3.1
$\text{Al}_2\text{O}_3$	406	0.23	8.75	3.0–4.5 <sup>55,56</sup>	3.2	2.9
$\text{B}_4\text{C}$	449	0.17	7.42	3.1–3.7 <sup>55</sup>	3.1	2.9
AlN	303	0.24	10.63	2.8 <sup>55</sup>	2.2	2.3
$\text{TiO}_2$	281	0.28	12.22	2.1–2.8 <sup>55,57</sup>	2.3	2.3
$\alpha$ - $\text{Si}_3\text{N}_4$	308	0.28	10.62	3.1 <sup>58</sup>	2.6	2.5
MgO	307	0.18	9.67	1.9–2.0 <sup>55</sup>	1.9	2.1
$\text{ThO}_2$	229	0.30	14.79	1.1 <sup>55</sup>	1.9	2.0
$\text{MgAl}_2\text{O}_4$	245	0.27	9.73	1.8–2.0 <sup>55</sup>	1.8	1.9
$\text{Y}_2\text{O}_3$	160	0.31	15.33	0.7 <sup>55</sup>	1.2	1.5
$\text{ZnO}_2$	158	0.27	10.15	1.6–2.5 <sup>55</sup>	0.9	1.4
Si	162	0.22	20.41	0.8–1.0 <sup>55</sup>	0.9	1.3
GaP	138	0.24	21.18	0.9 <sup>56</sup>	0.8	1.2
Ge	128	0.20	24.17	0.6 <sup>59</sup>	0.6	1.1
$\text{MgF}_2$	132	0.27	11.36	1.0 <sup>55</sup>	0.7	1.1
GaAs	116	0.24	23.92	0.4 <sup>60</sup>	0.6	1.0
$\text{BaTiO}_3$	117	0.29	13.15	1.1 <sup>55</sup>	0.7	1.0
InP	89	0.30	27.0	0.4–0.5 <sup>61</sup>	0.5	0.9
ZnS	86	0.32	20.21	0.7–1.0 <sup>55</sup>	0.5	0.8
ZnSe	73	0.29	23.60	0.3–1.0 <sup>56</sup>	0.4	0.7
CdS	51	0.36	26.07	0.3–0.8 <sup>62</sup>	0.3	0.8
CdSe	44	0.36	29.79	0.3–1.2 <sup>62</sup>	0.3	0.5
NaCl	37	0.25	22.6	0.2 <sup>63</sup>	0.1	0.3

**TABLE V.** Comparison between experimental fracture toughness  $K_{IC}$  and fracture toughness predicted by the current model and model of Niu<sup>10</sup> for a series of metals. The elastic properties and volume per atom  $V_0$  are calculated within the framework of density functional theory using the Perdew, Burke, and Ernzerhof (PBE) exchange-correlation functional<sup>13</sup> within the generalized gradient approximation and the projector-augmented wave method<sup>14</sup> as implemented in the Vienna *Ab Initio* Simulation Package (VASP).<sup>15,16</sup> The calculated Young's modulus  $E$  and Poisson's ratio  $\nu$  are determined within the Voigt-Reuss-Hill approximation.<sup>17</sup>

Material	Young's modulus $E$ (GPa)	Poisson's ratio $\nu$	$V_0$ (Å <sup>3</sup> /atom)	$K_{IC}^{exp}$ (MPa m <sup>1/2</sup> )	$K_{IC}^{calc}$ (MPa m <sup>1/2</sup> )	$K_{IC}^{Niu}$ (MPa m <sup>1/2</sup> )
Mg	62	0.27	22.87	16–18	17	20
Al	74	0.34	16.47	30–35	31	33
V	104	0.40	13.41	70–150	76	84
Ti	118	0.32	17.05	50–55	55	60
Ni	214	0.30	10.78	100–150	112	126
Fe <sup>a</sup>	243	0.29	11.97	120–150	132	123
Ag	81	0.37	17.67	40–105	44	34
Au	78	0.42	17.85	40–90	62	43
$\beta$ -Sn	55	0.30	28.4	15–30	17	22
Cu	134	0.35	11.94	40–100	76	55

<sup>a</sup>Ferromagnetic phase of Fe.

measuring the resulting area of indentation (Fig. 2). The Vickers hardness number  $H$  is then determined as

$$H = \frac{F}{A} \approx \frac{1.8544F}{d^2}, \quad (6)$$

where  $F$  is the force applied to the diamond,  $A$  is the surface area of the indentation, and  $d$  is the average length of the diagonal left by the indenter.

The model of Chen *et al.*<sup>5</sup> uses only the bulk modulus  $B$  and the shear modulus  $G$  to predict hardness. Although the connection between hardness and elastic properties may be arguable, they showed that the correlation between them is very high. However, the use of the bulk modulus  $B$  and shear modulus  $G$  is not very appropriate for deriving these dependencies because  $B$  and  $G$  have a strong correlation between themselves. The better choice of two elastic variables is Young's modulus  $E$  and Poisson's ratio  $\nu$

(Fig. 3), because these properties are less correlated with each other and thus expected to form a simpler expressions.

Rewriting the model obtained by Chen *et al.*<sup>5</sup> in terms of Young's modulus  $E$  and Poisson's ratio  $\nu$  using the homogeneous approximation

$$B = \frac{E}{3(1-2\nu)}; \quad G = \frac{E}{2(1+\nu)}, \quad (7)$$

we obtain the following formula for hardness:

$$H = 2 \left( \frac{9E(1-2\nu)^2}{8(1+\nu)^3} \right)^{0.585} - 3. \quad (8)$$

Therefore, the hardness can be well described in terms of some effective modulus  $E_{eff}$ , which characterizes the real

**TABLE VI.** Comparison between experimental fracture toughness  $K_{IC}$  and fracture toughness predicted by the current model and model of Niu<sup>10</sup> for a series of binary intermetallics. The elastic properties and volume per atom  $V_0$  are calculated within the framework of density functional theory using the Perdew, Burke, and Ernzerhof (PBE) exchange-correlation functional<sup>13</sup> within the generalized gradient approximation and the projector-augmented wave method<sup>14</sup> as implemented in the Vienna *Ab Initio* Simulation Package (VASP).<sup>15,16</sup> The calculated Young's modulus  $E$  and Poisson's ratio  $\nu$  are determined within the Voigt-Reuss-Hill approximation.<sup>17</sup> Electronegativity factors  $f_{EN}$  are obtained from Niu *et al.*<sup>10</sup>

Material	Young's modulus $E$ (GPa)	Poisson's ratio $\nu$	$V_0$ (Å <sup>3</sup> /atom)	Electronegativity factor $f_{EN}$	$K_{IC}^{exp}$ (MPa m <sup>1/2</sup> )	$K_{IC}^{calc}$ (MPa m <sup>1/2</sup> )	$K_{IC}^{Niu}$ (MPa m <sup>1/2</sup> )
Cu-Sn (3% Sn) <sup>a</sup>	148	0.32	12.25	1.00	40–80 <sup>55</sup>	73	57
Cu-Sn (9% Sn) <sup>a</sup>	122	0.30	12.94	1.00	40–80 <sup>55</sup>	50	43
Ni <sub>3</sub> Al	213	0.30	11.27	0.17	19–21 <sup>64</sup>	19	21
FeAl	241	0.27	11.78	0.13	17–25 <sup>65</sup>	15	18
Ti <sub>3</sub> Al	159	0.27	16.51	0.16	14–18 <sup>55</sup>	11	11
NiAl	188	0.31	12.02	0.10	6–7 <sup>66</sup>	10	9
TiAl	183	0.22	16.15	0.09	8 <sup>55</sup>	6	9
Al <sub>3</sub> Sc	156	0.18	17.32	0.09	4 <sup>67</sup>	4	6

<sup>a</sup>Tin bronze. See the calculation details in the work of Niu *et al.*<sup>10</sup>

**TABLE VII.** Predictions of hardness  $H_v$  and fracture toughness  $K_{IC}$  for some materials for which no experimental data were found. The elastic properties and volume per atom  $V_0$  are calculated within the framework of density functional theory using the Perdew, Burke, and Ernzerhof (PBE) exchange-correlation functional<sup>13</sup> within the generalized gradient approximation projector-augmented wave method<sup>14</sup> as implemented in the Vienna *Ab Initio* Simulation Package (VASP).<sup>15,16</sup> The calculated Young's modulus  $E$  and Poisson's ratio  $\nu$  are determined within Voigt-Reuss-Hill approximation.<sup>17</sup>

Material	Young's modulus $E$ (GPa)	Poisson's ratio $\nu$	$V_0$ ( $\text{\AA}^3/\text{atom}$ )	$H_v^{\text{calc}}$ (GPa)	$K_{IC}^{\text{calc}}$ ( $\text{MPa m}^{1/2}$ )
WB <sub>3</sub>	533	0.21	8.79	26.5 <sup>a</sup>	4.5
WB <sub>5</sub> <sup>b</sup>	620	0.15	8.79	45.2	4.7
CrB <sub>4</sub>	590	0.13	7.45	46.4	3.1
Fe <sub>3</sub> C	218	0.34	9.51	12.1	2.1
$\alpha$ -C <sub>3</sub> N <sub>4</sub>	784	0.16	82.19	54.4	10.5
$\beta$ -C <sub>3</sub> N <sub>4</sub>	772	0.18	87.32	47.3	10.8
Cubic - C <sub>3</sub> N <sub>4</sub>	874	0.13	41.31	68.7	7.5

<sup>a</sup>The experimental values are in the range of 28–43 GPa.<sup>68</sup>

<sup>b</sup>A superhard form of tungsten boride found in Ref. 69.

elastic tensor

$$E_{\text{eff}} = \chi(\nu)E, \quad (9)$$

where  $\chi(\nu)$  is a dimensionless function of Poisson's ratio.

This motivated us to search for a more accurate model and consider the following formula:

$$H = \gamma_0 E_{\text{eff}} = \gamma_0 \chi(\nu)E, \quad (10)$$

where  $\gamma_0$  is a dimensionless constant independent of the material.

$\chi(\nu)$  can be approximated by a rational function (Fig. 4). By fitting the experimental data we obtained  $\gamma_0 = 0.096$  and

$$\chi(\nu) = \frac{1 - 8.5\nu + 19.5\nu^2}{1 - 7.5\nu + 12.2\nu^2 + 19.6\nu^3}. \quad (11)$$

To ensure the correctness of the model, we plotted the relationship between the Vickers hardness and  $\chi(\nu)E$  (Fig. 5).

The results for covalent and ionic crystals are presented in Table I and for bulk metallic glasses in Table II. It is notable that the same formula describes all these materials.

Given the explicit role of Poisson's ratio in our model, we looked at some auxetic materials (i.e., those having a negative Poisson's ratio) and found that our model can make reasonable predictions for hardness (Table III).

## B. Fracture toughness

The model of fracture toughness is more speculative, because the experimental data are much more uncertain. Therefore, there are many ways to construct the model. However, we found a

**TABLE VIII.** Predictions of hardness  $H_v$  and fracture toughness  $K_{IC}$  for some materials obtained from Ref. 73. The elastic properties and volume per atom  $V_0$  are calculated within the framework of density functional theory using the Perdew, Burke, and Ernzerhof (PBE) exchange-correlation functional<sup>13</sup> within the generalized gradient approximation projector-augmented wave method<sup>14</sup> as implemented in the Vienna *Ab Initio* Simulation Package (VASP).<sup>15,16</sup> The calculated Young's modulus  $E$  and Poisson's ratio  $\nu$  are determined within Voigt-Reuss-Hill approximation.<sup>17</sup>

Material	Young's modulus $E$ (GPa)	Poisson's ratio $\nu$	$V_0$ ( $\text{\AA}^3/\text{atom}$ )	$H_v^{\text{calc}}$ (GPa)	$K_{IC}^{\text{calc}}$ ( $\text{MPa m}^{1/2}$ )
BP	364	0.12	11.75	29.4	1.5
Cr <sub>2</sub> B	439	0.23	9.33	20.3	3.6
Cr <sub>2</sub> C	457	0.24	9.38	21.0	4.0
Cr <sub>5</sub> B <sub>3</sub>	453	0.20	9.14	24.0	3.4
Cr <sub>7</sub> C <sub>3</sub>	275	0.31	9.34	14.6	2.5
CrB	495	0.19	8.35	28.2	3.8
CrB <sub>4</sub>	573	0.13	7.37	45.0	2.8
CrB <sub>5</sub>	489	0.17	7.55	32.0	3.6
Hf <sub>6</sub> B	158	0.27	19.83	7.7	1.0
HfB <sub>10</sub>	438	0.18	7.79	26.8	3.1
HfB <sub>12</sub>	421	0.20	7.74	22.3	3.0
HfB <sub>2</sub>	454	0.13	10.66	35.7	2.3
MoB	527	0.25	10.14	24.5	5.2
MoB <sub>2</sub>	534	0.23	8.87	24.7	4.8
MoB <sub>3</sub>	523	0.17	9.26	34.2	4.1
ReB <sub>2</sub>	639	0.18	9.21	39.1	5.6
Ti <sub>5</sub> B <sub>4</sub>	354	0.17	11.48	23.2	2.4
Ti <sub>5</sub> B <sub>6</sub>	467	0.14	10.10	35.5	2.5
Ti <sub>7</sub> B <sub>2</sub>	167	0.28	14.46	8.3	1.1
TiB	439	0.15	10.87	32.0	2.8
TiB <sub>2</sub>	578	0.12	8.80	46.7	2.9
TiSi <sub>2</sub>	278	0.18	14.14	17.0	1.7
W <sub>2</sub> B	399	0.30	12.34	20.8	4.5
W <sub>4</sub> B <sub>3</sub>	513	0.24	11.54	23.6	5.0
W <sub>4</sub> B <sub>7</sub>	597	0.19	9.71	34.0	5.2
WB <sub>2</sub>	588	0.19	9.60	33.5	5.0
WB <sub>4</sub>	522	0.21	8.32	26.0	4.6
Zr <sub>3</sub> B <sub>2</sub>	194	0.26	15.58	9.2	1.3
ZrB <sub>12</sub>	479	0.16	7.82	33.2	3.3
ZrB <sub>2</sub>	519	0.14	10.35	39.4	3.0
ZrB <sub>4</sub>	522	0.14	8.88	39.7	3.0
$\alpha$ -WB	486	0.27	10.45	23.6	4.9
$\beta$ -WB	474	0.24	10.45	21.8	4.2
TaB	510	0.21	11.33	25.4	4.4
VB	541	0.18	9.04	33.1	4.3
VB <sub>12</sub>	525	0.14	7.12	39.9	3.2

similar approach to work well

$$K_{IC} = \alpha_0^{-1/2} V_0^{1/6} [\zeta(\nu)E]^{3/2}, \quad (12)$$

where  $\alpha_0$  depends on chemical bonding in the material and has

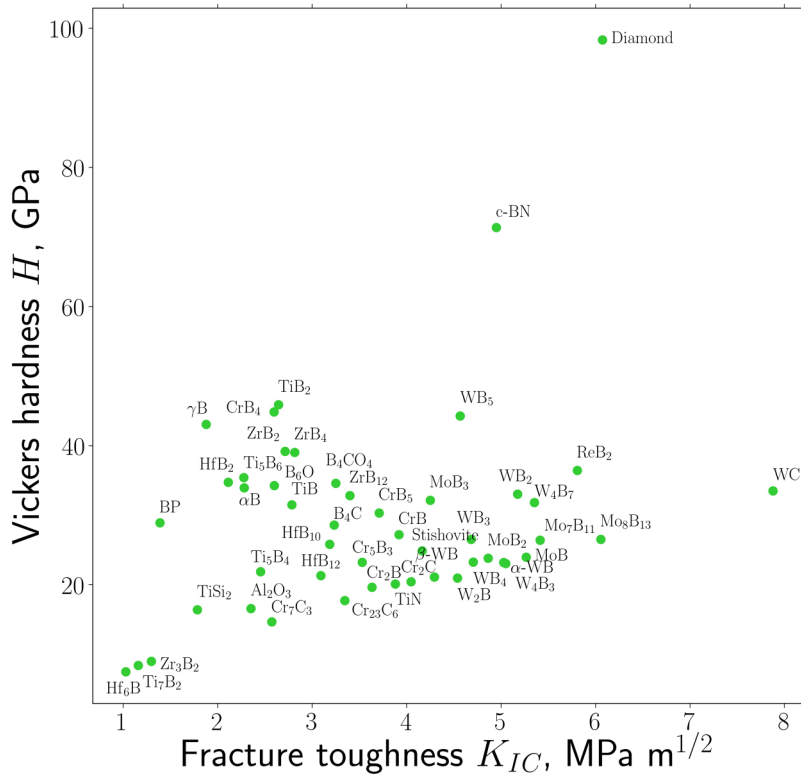


FIG. 7. Ashby plot of Vickers hardness vs fracture toughness for various materials calculated by the current model.

units of pressure,  $V_0$  is the volume per atom, and  $\zeta(\nu)$  is a dimensionless function of Poisson's ratio.

By fitting the experimental data for covalent and ionic crystals (Fig. 6), we obtained  $\alpha_0 = 8840$  GPa and

$$\zeta(\nu) = \frac{1 - 13.7\nu + 48.6\nu^2}{1 - 15.2\nu + 70.2\nu^2 - 81.5\nu^3}. \quad (13)$$

The results are presented in Table IV.

The same model can be applied for pure metals. In this case,  $\alpha_0 = 2$  GPa, much smaller, and  $\zeta(\nu)$  remains the same. Results for metals are given in Table V.

In the case of intermetallics (two or more elements with metallic bonding), it is necessary to introduce the electronegativity factor  $f_{EN}$  as in Eq. (4). This factor characterizes the tendency of electrons to form localized states centered on the more electronegative atoms. If the electrons are localized, we expect a low fracture toughness. Therefore, we use the following formula for intermetallics:

$$K_{IC} = f_{EN} \alpha_0^{-1/2} V_0^{1/6} [\zeta(\nu) E]^{3/2}. \quad (14)$$

The results for intermetallics are presented in Table VI.

### III. CONCLUSIONS

Motivated by finding that Young's and Poisson's moduli are less correlated and, therefore, serve as more natural elastic variables, we developed new models of hardness and fracture toughness, which display very good agreement with experiment. The empirical, but physically motivated formulas, which we obtained, are surprisingly accurate and can facilitate the development of theoretical models. Although hardness and fracture toughness are determined not only by elastic deformations, we clearly showed that a good correlation can be established. The relationship between the hardness and elasticity can be traced via the crystal structure. In particular, some of this relation is on Poisson's ratio and indeed its connection to structure related properties including elastic anisotropy and packing density is well known.<sup>70</sup> This also agrees with previously established results that plastic deformations can be correlated with Poisson's ratio.<sup>71</sup> Roughly speaking, Young's modulus characterizes overall strength of bonds while Poisson's ratio relates to chemical bonding. In particular, it has high values for metals and can serve as an indicator of ductile behavior.<sup>72</sup>

Using analytical models proposed here, we made predictions for some materials with unknown experimental hardness and fracture toughness (Table VII). We also calculated the values for data obtained from Ref. 73 (Table VIII). Ashby plot of the Vickers hardness vs fracture toughness for these and other materials is presented

in Fig. 7. This plot can be used to find materials with the desired combination of properties.

## ACKNOWLEDGMENTS

We thank the Russian Science Foundation for support (Grant No. 19-72-30043).

## REFERENCES

- 1I. Maslenikov, A. Useinov, A. Birykov, and V. Reshetov, "Reducing the influence of the surface roughness on the hardness measurement using instrumented indentation test," *IOP Conf. Ser. Mater. Sci. Eng.* **256**, 012003 (2017).
- 2C. M. Sung and M. Sung, "Carbon nitride and other speculative super hard materials," *Mater. Chem. Phys.* **43**, 1–18 (1996).
- 3A. R. Oganov and A. O. Lyakhov, "Towards the theory of hardness of materials," *J. Superhard Mater.* **32**, 143 (2010).
- 4D. M. Teter, "Computational alchemy: The search for new superhard materials," *MRS Bull.* **23**(1), 22–27 (1998).
- 5X. Chen, H. Niu, D. Li, and Y. Li, "Modeling hardness of polycrystalline materials and bulk metallic glasses," *Intermetallics* **19**, 1275–1281 (2011).
- 6F. Gao, J. He, E. Wu, S. Liu, D. Yu, D. Li, S. Zhang, and Y. Tian, "Hardness of covalent crystals," *Phys. Rev. Lett.* **91**, 015502 (2003).
- 7A. Šimůnek and J. Vackář, "Hardness of covalent and ionic crystals: First-principle calculations," *Phys. Rev. Lett.* **96**, 085501 (2006).
- 8K. Li, X. Wang, F. Zhang, and D. Xue, "Electronegativity identification of novel superhard materials," *Phys. Rev. Lett.* **100**, 235504 (2008).
- 9A. O. Lyakhov and A. R. Oganov, "Evolutionary search for superhard materials: Methodology and applications to forms of carbon and TiO<sub>2</sub>," *Phys. Rev. B* **84**, 092103 (2011).
- 10H. Niu, S. Niu, and A. R. Oganov, "Simple and accurate model of fracture toughness of solids," *J. Appl. Phys.* **125**, 065105 (2019).
- 11L. C. Allen, "Electronegativity is the average one-electron energy of the valence-shell electrons in ground-state free atoms," *J. Am. Chem. Soc.* **111**, 9003 (1989).
- 12A. R. Franco, Jr., G. Pintaude, A. Sinatora, C. E. Pinedo, and A. P. Tschiptschin, "The use of a Vickers indenter in depth sensing indentation for measuring elastic modulus and Vickers hardness," *Mater. Res.* **7**(3), 483–491 (2004).
- 13J. P. Perdew, K. Burke, and M. Ernzerhof, "Generalized gradient approximation made simple," *Phys. Rev. Lett.* **77**, 3865 (1996).
- 14P. E. Blochl, "Projector augmented-wave method," *Phys. Rev. B* **50**, 17953 (1994).
- 15G. Kresse and J. Hafner, "Ab initio molecular dynamics for liquid metals," *Phys. Rev. B* **47**, 558(R) (1993).
- 16G. Kresse and J. Furthmüller, "Efficient iterative schemes for ab initio total-energy calculations using a plane-wave basis set," *Phys. Rev. B* **54**, 11169 (1996).
- 17R. Hill, "The elastic behaviour of a crystalline aggregate," *Proc. Phys. Soc.* **65**, 349 (1952).
- 18R. A. Andrievski, "Superhard materials based on nanostructured high-melting point compounds: Achievements and perspectives," *Int. J. Refract. Met. Hard Mater.* **19**, 447 (2001).
- 19V. L. Solozhenko, D. Andrault, Y. L. Godec, and M. Mezouar, "Ultimate metastable solubility of boron in diamond: Synthesis of superhard diamondlike BC<sub>5</sub>," *Phys. Rev. Lett.* **102**, 015506 (2009).
- 20*The Science of Hardness Testing and its Research Applications*, edited by J. H. Westbrook and H. Conrad (American Society for Metals, Materials Park, Ohio, 1973).
- 21V. L. Solozhenko, O. O. Kurakevych, and A. R. Oganov, "On the hardness of a new boron phase, orthorhombic  $\gamma$ -B<sub>28</sub>," *J. Superhard Mater.* **30**, 428 (2008).
- 22V. Domnich, S. Reynaud, R. A. Haber, and M. Chhowalla, "Boron carbide: Structure, properties, and stability under stress," *J. Am. Ceram. Soc.* **94**(11), 3605–3628 (2011).
- 23D. W. He, Y. S. Zhao, L. Daemen, J. Qian, D. T. Shen, and T. W. Zerdar, "Boron suboxide: As hard as cubic boron nitride," *Appl. Phys. Lett.* **81**, 643–645 (2002).
- 24I. Yonenaga and T. Suzuki, "Indentation hardnesses of semiconductors and a scaling rule," *Philos. Mag. Lett.* **82**, 535–542 (2002).
- 25S. G. Huang, K. Vanmeensel, O. Van der Biest, and J. Vleugels, "Binderless WC and WC-VC materials obtained by pulsed electric current sintering," *Int. J. Refract. Met. H* **26**, 41–47 (2008).
- 26M. Hebbache, L. Stuparević, and D. Živković, "A new superhard material: Osmium diboride OsB<sub>2</sub>," *Solid State Commun.* **139**(5), 227–231 (2006).
- 27F. Fernandes, T. Christiansen, K. Dahl, and M. Somers, "Growth of vanadium carbide by halide-activated pack diffusion," in *Proceedings of Heat Treatment and Surface Engineering* (2013), pp. 295–301.
- 28Q. Gu, G. Krauss, and W. Steurer, "Transition metal borides: Superhard versus ultra-incompressible," *Adv. Mater.* **20**(19), 3620–3626 (2008).
- 29D. Ferro, S. M. Barinov, J. V. Rau, A. Latini, R. Scandurra, and B. Brunetti, "Vickers and Knoop hardness of electron beam deposited ZrC and HfC thin films on titanium," *Surf. Coat. Technol.* **200**, 4701–4707 (2006).
- 30S. Cardinal, A. Malchere, V. Garnier, and G. Fantozzi, "Microstructure and mechanical properties of TiC-TiN based cermets for tools application," *Int. J. Refract. Met. H* **27**, 521–527 (2009).
- 31L. Čurković, V. Rede, K. Grilec, and A. Mulabdić, "Hardness and fracture toughness of alumina ceramics," in *Proceedings of the Conference on Materials, Processes, Friction and Wear, Vela Luka, Croatia* (Croatian Society for Materials and Tribology, 2007).
- 32J. Chen, V. V. Struzhkin, Z. Wu, M. Somayazulu, J. Qian, S. Kung, A. N. Christensen, Y. Zhao, R. E. Cohen, H. Mao, and R. J. Hemley, "Hard superconducting nitrides," *Proc. Natl. Acad. Sci. U.S.A.* **102**(9), 3198–3201 (2005).
- 33A. Nino, A. Tanaka, S. Sugiyama, and H. Taimatsu, "Indentation size effect for the hardness of refractory carbides," *Mater. Trans.* **51**, 1621–1626 (2010).
- 34M. D. Drory, J. W. Ager III, T. Suski, I. Grzegory, and S. Porowski, "Hardness and fracture toughness of bulk single crystal gallium nitride," *Appl. Phys. Lett.* **69**, 4044–4046 (1996).
- 35S. E. Grillo, M. Ducarroir, M. Nadal, E. Tournie, and J. P. Fanrie, "Nanoindentation of Si, GaP, GaAs and ZnSe single crystals," *J. Phys. D Appl. Phys.* **35**(1), 3015 (2002).
- 36V. Domnich, Y. Aratyn, W. M. Kriven, and Y. Gogotsi, "Temperature dependence of silicon hardness: Experimental evidence of phase transformation," *Rev. Adv. Mater. Sci.* **17**, 33–41 (2008).
- 37I. Yonenaga, Y. Ohkubo, M. Deura, K. Kutsukake, Y. Tokumoto, Y. Ohno, A. Yoshikawa, and X. Q. Wang, "Elastic properties of indium nitrides grown on sapphire substrates determined by nano-indentation: In comparison with other nitrides," *AIP Adv.* **5**(7), 077131 (2015).
- 38R. K. Banerjee and P. Feltham, "Deformation and fracture of germanium single crystals," *J. Mater. Sci.* **9**, 1478–1482 (1974).
- 39T. H. Fang, W. J. Chang, and C. M. Lin, "Nanoindentation characterization of ZnO thin films," *Mater. Sci. Eng. A* **452–453**, 715 (2006).
- 40J. W. Cha, S. C. Hwang, and E. S. Lee, "Evaluation of Y<sub>2</sub>O<sub>3</sub> surface machinability using ultra-precision lapping process with IED," *J. Mech. Sci. Technol.* **23**, 1194–1201 (2009).
- 41A. K. M. A. Shawon and S.-C. Ur, "Mechanical and thermoelectric properties of bulk AlSb synthesized by controlled melting, pulverizing and subsequent vacuum hot pressing," *Appl. Sci.* **9**, 1609 (2019).
- 42D. Maske, M. Deshpande, R. Choudhary, and D. Gadkari, "Lattice constant and hardness of InSb:Bi bulk crystals grown by vertical directional solidification," *AIP Conf. Proc.* **1728**, 020496 (2016).
- 43A. Chmel, A. Dunaev, I. Shcherbakov, and A. Sinani, "Luminescence from impact- and abrasive-damaged ZnS ceramics," *Proc. Str. Int.* **9**, 3–8 (2018).
- 44A. S. Borshevski, N. A. Goryunova, and N. K. Takhtare, "Investigation of the microhardness of some semiconductors with a structure of sphalerite," *J. Tech. Phys.* **27**, 1408–1413 (1957).
- 45*Handbook of Chemistry and Physics*, 85 ed., edited by D. R. Lide (CRC Press, 2004), Vol. 85.

- <sup>46</sup>L. I. Berger, *Semiconductor Materials* (CRC Press, 1996), p. 125.
- <sup>47</sup>C. Ascheron, H. Neumann, G. Kühn, and C. Haase, "Microhardness of ZnSe and its change by proton implantation," *Cryst. Res. Technol.* **24**(12), 1275–1279 (1989).
- <sup>48</sup>V. Keryvin, V. H. Hoang, and J. Shen, "Hardness, toughness, brittleness and cracking systems in an iron-based bulk metallic glass by indentation," *Intermetallics* **17**, 211–217 (2009).
- <sup>49</sup>W. H. Wang, "Correlations between elastic moduli and properties in bulk metallic glasses," *J. Appl. Phys.* **99**, 093506 (2006).
- <sup>50</sup>D. H. Xu, G. Duan, W. L. Johnson, and C. Garland, "Formation and properties of new Ni-based amorphous alloys with critical casting thickness up to 5 mm," *Acta Mater.* **52**, 3493–3497 (2004).
- <sup>51</sup>Y. Zhang, D. Q. Zhao, M. X. Pan, and W. H. Wang, "Glass forming properties of Zr-based bulk metallic alloys," *J. Non-Cryst. Solids* **315**, 206–210 (2003).
- <sup>52</sup>S. Li, R. J. Wang, M. X. Pan, D. Q. Zhao, and W. H. Wang, "Formation and properties of RE<sub>55</sub>Al<sub>25</sub>Co<sub>20</sub> (RE = Y, Ce, La, Pr, Nd, Gd, Tb, Dy, Ho and Er) bulk metallic glasses," *J. Non-Cryst. Solids* **354**, 1080 (2008).
- <sup>53</sup>J. Dagdelen, J. Montoya, M. De Jong, and K. Persson, "Computational prediction of new auxetic materials," *Nat. Commun.* **8**, 323 (2017).
- <sup>54</sup>D. M. Hatch, S. Ghose, and J. L. Bjorkstam, "The  $\alpha$ - $\beta$  phase transition in AlPO cristobalite: Symmetry analysis, domain structure and transition dynamics," *Phys. Chem. Miner.* **21**, 67–77 (1994).
- <sup>55</sup>R. G. Munro, S. W. Freiman, and T. L. Baker, *Fracture Toughness Data for Brittle Materials* (NIST, 1998).
- <sup>56</sup>M. Weber, *Handbook of Optical Materials, Laser and Optical Science and Technology* (Taylor and Francis, 2002).
- <sup>57</sup>G. Anstis, P. Chantikul, B. R. Lawn, and D. Marshall, "A critical evaluation of indentation techniques for measuring fracture toughness I, direct crack measurements," *J. Am. Ceram. Soc.* **64**, 539 (1981).
- <sup>58</sup>I. Tanaka, H.-J. Kleebe, M. K. Cinibulk, J. Bruley, D. R. Clarke, and M. Rühle, "Calcium concentration dependence of the intergranular film thickness in silicon nitride," *J. Am. Ceram. Soc.* **77**, 911 (1994).
- <sup>59</sup>P. Lemaître, "Fracture toughness of germanium determined with the Vickers indentation technique," *J. Mater. Sci. Lett.* **7**, 895 (1998).
- <sup>60</sup>G. Michot, A. George, A. Chabli-Brenac, and E. Molva, "Fracture toughness of pure and in-doped GaAs," *Scr. Metal.* **22**, 1043 (1988).
- <sup>61</sup>F. Ericson, S. Johansson, and J. A. Schweitz, "Hardness and fracture toughness of semiconducting materials studied by indentation and erosion techniques," *Mater. Sci. Eng. A* **105**, 131 (1988).
- <sup>62</sup>M. J. Tafreshi, K. Balakrishnan, and R. Dhanasekaran, "Microhardness and optical studies on CdS single crystals grown by sublimation and hydrogen transport techniques," *Mater. Res. Bull.* **30**, 1387 (1995).
- <sup>63</sup>N. Nrita, K. Higashida, and S. Kitano, "Dislocation distribution around a crack tip and the fracture toughness in NaCl crystals," *Scr. Metal.* **21**, 1273 (1987).
- <sup>64</sup>J. D. Rigney and J. J. Lewandowski, "Fracture toughness of monolithic nickel aluminide intermetallics," *Mater. Sci. Eng. A* **149**, 143 (1992).
- <sup>65</sup>P. Specht and P. Neumann, "Fracture planes and toughness of stoichiometric FeAl single crystals," *Intermetallics* **3**, 365 (1995).
- <sup>66</sup>J. Ast, B. Merle, K. Durst, and M. Goken, "Fracture toughness evaluation of NiAl single crystals by microcantilevers—A new continuous J-integral method," *J. Mater. Res.* **31**, 3786 (2016).
- <sup>67</sup>W. Gerberich, S. Venkataraman, J. Hoehn, and P. Marsh, *Structural Intermetallics* (TMS, Warrendale, PA, 1993).
- <sup>68</sup>X. Y. Cheng, X. Q. Chen, D. Z. Li, and Y. Y. Li, "Computational materials discovery: The case of the W-B system," *Acta Cryst. C* **70**, 85 (2014).
- <sup>69</sup>A. G. Kvashnin, H. A. Zakaryan, C. Zhao, Y. Duan, Y. A. Kvashnina, C. Xie, H. Dong, and A. R. Oganov, "New tungsten borides, their stability and outstanding mechanical properties," *J. Phys. Chem. Lett.* **9**, 3470–3477 (2018).
- <sup>70</sup>G. N. Greaves, A. L. Greer, R. S. Lakes, and T. Rouxel, "Poisson's ratio and modern materials," *Nat. Mat.* **10**, 823 (2011).
- <sup>71</sup>D. P. Wang, D. Q. Zhao, D. W. Ding, H. Y. Bai, and W. H. Wang, "Understanding the correlations between Poisson's ratio and plasticity based on microscopic flow units in metallic glasses," *J. Appl. Phys.* **115**(12), 123507 (2014).
- <sup>72</sup>S. F. Pugh, "Relations between the elastic moduli and the plastic properties of polycrystalline pure metals," *Philos. Mag.* **45**, 823–843 (1954).
- <sup>73</sup>A. G. Kvashnin, Z. Allahyari, and A. R. Oganov, "Computational discovery of hard and superhard materials," *J. Appl. Phys.* **126**(4), 040901 (2019).